# Disclaimer

This note has not been internally reviewed by the DØ Collaboration. Results or plots contained in this note were only intended for internal documentation by the authors of the note and they are not approved as scientific results by either the authors or the DØ Collaboration. All approved scientific results of the DØ Collaboration have been published as internally reviewed Conference Notes or in peer reviewed journals.

DØ Note 2806

# The DØ silicon tracker

W. E. Cooper [1]
*Fermi National Accelerator Laboratory, P.O. Box 500, Batavia, IL 60510, USA*

For the DØ Collaboration

**Abstract**

The upgrade of the DØ detector for Run II of the Fermilab collider includes a silicon tracker, a new scintillating fiber based central tracking system, a 2 Tesla superconducting solenoid, and scintillator-based preshower detectors. The design and predicted performance of the silicon tracker are described.

Presented at Beauty 95, Oxford, U.K.
To be published in NIM A as part of the proceedings.

[1] cooper@fnalv.fnal.gov

# 1 The DØ Detector Upgrade

The DØ detector will be upgraded for Run II of the Fermilab collider in order to optimize its physics capabilities in the Fermilab Main Injector era. The existing detector, which has been used during Run I of the collider, has been described previously[1]. The upgraded detector[2][3][4], shown in Figure 1, builds upon the strengths of the present detector. A 2 Tesla superconducting solenoid having a 1066 mm inside diameter and a coil length of 2556 mm allows charged particle momentum measurements which complement the energy measurements of the central and end liquid argon calorimeters. A central preshower detector will be added to restore the loss in electromagnetic energy resolution which would otherwise occur from the addition of the magnet. Along with new end preshower detectors, the central preshower detector also improves electron identification. The existing inter-cryostat detectors, which compensate for energy loss in cryostat walls, will be modified to match the new geometry and to relocate photomultiplier tubes to a region of acceptably low magnetic field.

The expected accelerator operating parameters for Run II, summarized in Table 1, have prompted detector improvements in several areas. The overall trigger framework will be replaced for Run II. The calorimeter electronics will be upgraded to match the reduced bunch crossing time and increased luminosity. The peak sampling time will be reduced to 400 ns to match the charge drift time in the calorimeter and the expected minimum bunch spacing at the beginning of Run II. New preamplifiers with low-noise FET's and increased drive capability will be used to compensate for the higher sensitivity to noise associated with the shorter sampling time. Cabling will be replaced to match the impedance of cabling within the cryostats and the input impedance of the new preamplifiers. Dual-pipeline shaper circuitry will be used to provide deadtimeless readout and allow sufficient time for a trigger decision to be made.

The muon system triggering and front-end electronics systems will be replaced to obtain the improved triggering rejection power needed with the higher Run II luminosity. The forward muon chambers will be replaced with an Iarocci tube system designed for the increased luminosity.

Finally, the central tracking system, which has served us well during Run I, will be replaced entirely by scintillating fiber and silicon tracker systems[5]. Scintillating fiber barrels with visible light photon counter (VLPC) photode-

tection occupy the region 200 mm < r < 500 mm and | z | < 1200 mm. The optimum layer structure of the 0.835 mm diameter fibers is under study. Our present design includes 16 doublet layers, arranged in "superlayers": 8 layers with fibers parallel to the beamline and the remaining layers with stereo angles of $\pm 1.5°$ to $\pm 3.0°$. All fiber doublet layers are constructed so that one layer is offset by one half the $\approx$900 $\mu$m fiber spacing with respect to its partner in order to remove gaps in coverage and improve the doublet position resolution.

The region r < 180 mm is occupied by a new, $800000^+$ channel silicon tracker, its support structure, cooling manifolding, and cabling. Larger radius "H-disks" at the ends of the tracking region overlap the radius of the innermost fiber layers and extend tracking coverage to slightly above $| \eta | = 3$. The silicon system significantly improves position resolution, improves the momentum resolution obtained with the scintillating fiber tracker and muon systems, and provides the ability to reconstruct separated vertices.

# 2 Overview of the silicon tracker design

The silicon tracker is based upon seven barrel modules with silicon parallel to the beamline, twelve "F-disks" with silicon normal to the beamline, and four sets of "H-disks" with silicon normal to the beamline. The 889 mm long central barrel region provides four layers of r-$\phi$ tracking to $\eta \approx 2.2$ for tracks from the center of the interaction region and to $\eta \approx 1.6$ for tracks originating 1 $\sigma$ from the center. Two of the barrel layers provide small angle stereo tracking in conjunction with the scintillating fiber tracker. Six of the double-sided F-disks are placed between barrel modules to provide 3-dimensional tracking and to improve tracking at higher $\eta$. The remaining F-disks are divided evenly between the two ends of the barrel region. The H-disks extend forward coverage to match that of the end calorimeters.

The barrel modules and F-disks are supported by a double-walled carbon-fiber/epoxy half-cylinder from the ends of the innermost scintillating fiber layer. The half-cylinder aids in maintaining precise relative alignment within this portion of the silicon, locates the silicon relative to the scintillating fibers, and supports silicon cabling and cooling services. Separate carbon-fiber/epoxy covers for each module enclose the top half of silicon modules, allow access to modules during detector assembly, and support cabling on

the top half of the detector. Compensation will be made for the predicted 120 $\mu$m deflection of the half-cylinder as modules are aligned. Full carbon-fiber/epoxy end disk closures of the half-cylinder region, in conjunction with the scintillating fiber barrels, provide a quasi-hermetic, light-free environment. Measurements have established that a sufficiently low dew point to prevent condensation is obtained by flowing a fraction of a liter per hour of dry gas into this region. The enclosures and support systems for the H-disks remain to be designed.

The modular construction of the silicon detector provides flexibility in fabricating, debugging, and servicing the detector. Those disks between barrels will be attached to one of the barrels to form a barrel/disk module. The sets of F-disks at each end of the barrels will also be joined into modules. Each module will be supported from the half-cylinder with a set of kinematic mounts at 3, 6, and 9 o'clock. The 3 and 9 o'clock mounts establish vertical position, position along the beamline, and azimuthal orientation. The 6 o'clock mount positions horizontally. This kinematic mount system allows thermal contraction toward the beamline as the silicon is cooled while maintaining the angular orientations and central positions of the modules.

All silicon in the present design has a thickness of 300 $\mu$m. A combination of single-sided (traces on one surface) and double-sided (traces on both surfaces) silicon has been ordered from Micron Semiconductor, Inc. Prototype quantities of the single-sided silicon have been received, tested by personnel from the University of California at Riverside, the University of Oklahoma, and Fermilab and found to perform well. The masks for the double-sided silicon are under design by UCR and Micron Semiconductor.

The purchase contract for F-disk double-sided silicon is under negotiation. Prototype silicon for the F-disks was obtained from Micron Semiconductor in 1993. Irradiation tests of prototype wedges for the F-disks at Triumph last May suggest that changes in the mask/detector design may be needed in order to obtain improved radiation hardness. The design of the single-sided silicon for the H-disks is well underway at Moscow State University.

# 3 Silicon modules

Each barrel module contains 72 "ladders" 120.125 mm long. As indicated in Figure 2 and Table 2, the ladders are arranged in four layers, each with an

inner and an outer sublayer. Ladder locations have been chosen to ensure azimuthal overlap of inner and outer sublayers and to allow the use of only two basic ladder types: 21.2 mm wide single-sided ladders in layers 1 and 3 and 34.0 mm wide double-sided ladders in layers 2 and 4.

Each ladder includes two 60 mm long rectangular wafers of silicon positioned end-to-end and joined electrically by wirebonds. The wafers are held in relative position by two longitudinal rails each consisting of a carbon/boron fiber, Rohacell, carbon/boron fiber sandwich. Thermal bowing has been minimized by choosing the mixture of carbon and boron fibers so that the thermal expansion coefficient of the rails matches that of silicon.

Ladders are supported and positioned by an active, 9.525 mm thick, cooled beryllium bulkhead and a passive, 0.75 mm thick, uncooled beryllium bulkhead. External support is provided by kinematic mounts at the active bulkhead only for several reasons. First, the positions and orientations of modules are better controlled from the active bulkhead because the barrel diameter (200 mm) is significantly greater than the barrel length (120 mm). Second, all external cabling and services come to the active bulkhead end of the module and the effects of their loadings are minimized. Third, thermal contraction problems are minimized by supporting the passive bulkhead via the ladders themselves. Thus the active bulkhead sets absolute positions of ladders at one end and the passive bulkhead sets relative positions of ladders at the other end.

This design approach requires that a fraction of the ladders be rigidly attached to bulkheads. All ladders are held against bulkhead mounting surfaces with a post and pin arrangement which also establishes ladder lateral positions. Structural requirements are met by fastening the layer 2 and 4 layer ladders to bulkheads with epoxy as well: thermally and electrically conductive epoxy at the active bulkhead and unfilled epoxy at the passive bulkhead. A thermal connection to the active bulkhead for the layer 1 and 3 ladders is provided with thermal grease. This approach simplifies the replacement of layer 1 ladders should they sustain excessive radiation damage. Our goal is to maintain a ladder positioning accuracy of $\pm 10$ $\mu$m in the transverse (phi) direction, $\pm 50$ $\mu$m in the radial direction, and $\pm 75$ $\mu$m in the longitudinal direction.

We have chosen to use SVX-II chips, rather than SVX-III chips, for ladder readout because their development schedule better matches our detector fabrication schedule and because their smaller size permits a reduction in

ladder mass and a more favorable bulkhead geometry. The chips and associated readout components are mounted on a kapton-base flex-circuit (high density interconnect, or HDI) at one end of the ladder. Our baseline design includes transceivers on the ladders for input and output signals. Beryllium substrates are used to provide a thermal path from readout heat sources to coolant passages, to maintain flatness at that end of the ladder, and to provide ladder positioning features. Studies are in progress to understand whether the transceiver functions can be incorporated into the SVX-II chips.

Our double-sided ladder design with two 300 $\mu$m thick beryllium substrates is shown in Figure 3. SVX chips and other readout components are mounted on an HDI which wraps around one ladder edge and services both ladder surfaces. The required barrel-to-barrel separation is reduced by making electrical connections at ladder edges with kapton-based flatline and passing the flatlines between ladders to the outer radius of the detector support half-cylinder and its upper covers. Cabling to the outside world passes along the exterior of the half-cylinder and its covers. The single-sided ladder design is similar, but has readout components on only the ladder surface away from the bulkhead.

Single-sided ladders with a trace pitch of 50 $\mu$m and traces parallel to the beamline are used in barrel layers 1 and 3. Three SVX-II chips are used to read out each of the single-sided ladders. Double-sided, stereo-readout ladders with a trace pitch of 50 $\mu$m on the p-side and 65 $\mu$m on the n-side are used in barrel layers 2 and 4. The wider 65 $\mu$m pitch is necessary to provide sufficient space between implants in the microbond pad region. Five SVX-II readout chips are used on the p-side and four on the n-side. The p-side traces run parallel to the beamline and the n-side traces run at and angle of 2° from the beamline.

The SVX-II readout structure is mounted outboard of the cooled bulkhead in order to minimize the portion of a ladder heated. Beryllium substrates support the HDI and provide a thermal path from heat sources to the cooled bulkhead. Studies are in progress to understand the benefits of adding a layer of CVD diamond, which has a thermal conductivity about 6 times that of beryllium, between one beryllium substrate and the silicon. This would improve the thermal conduction path from SVX-II chips and transceivers near the end of the ladder and decrease the maximum silicon temperature. The improvement has been estimated by calculating the longitudinal temperature distribution of a ladder in which one of the 300$\mu$m thick

beryllium substrates has been replaced entirely with a 200 $\mu$m thick layer of CVD diamond. The result is shown in Figure 4. The highest silicon temperature is approximately 12°C above the coolant temperature. This result is conservative in that both beryllium substrates would be retained in ladders to minimize thermal bowing.

Two types of disks are used in the detector: F-disks comprised of twelve overlapping wedges with active area extending between r = 25.4 mm and r = 98.4 mm and H-disks comprised of 24 overlapping wedge sectors with active area extending between r = 96 mm and r = 236 mm. The wedges of the F-disks are supported by a 2.5 mm thick by 15.7 mm wide cooling channel with a dodecagonal outline. Wedges are mounted from alternate faces of the cooling channel as indicated in Figure 5. The F-disk wedge silicon is double-sided and provides 30° stereo with traces on opposite surfaces at $\pm$15° from the wedge centerline. By mounting the readout structure outboard of the silicon, we are able to limit the effective disk thickness to 6 mm and the barrel-to-barrel separation to 8 mm. On the surface of a wedge facing the cooling channel, a flex-circuit jumper is used for connections from the silicon to the SVX-II chips. This mounting arrangement has the additional advantage that heat from power dissipation in the readout structure is intercepted by the cooling channel before reaching the silicon.

The structure of H-disks is similar to that of F-disks, but includes some ladder features. The size of silicon available requires that each H-disk be divided into 24 azimuthal sectors, each containing a smaller radius and a larger radius silicon wedge. The two wedges are joined electrically with wirebonds and mechanically with rails to form an H-disk sector. As in the F-disks, readout, cooling, and mechanical support are provided near the disk outer radius. H-disk silicon is single-sided with a trace pitch of 40 $\mu$m and a readout pitch of 80 $\mu$m. Traces run at an angle of 7.5° from the centerline of a wedge, i.e., parallel to one wedge edge. Pairs of H-disks are formed into back-to-back sets to provide a stereo angle of 15°.

The silicon cooling system has been conservatively designed assuming a power dissipation of 0.64 watts per SVX-II chip and associated readout components, a coolant temperature rise of 1°C along any detector coolant path, and a deionized, ethylene glycol - water coolant. The design power dissipation is shown in Table 3. Two fully redundant chillers have been purchased, each capable of removing 6600 watts at $-10$°C. All portions of the cooling system in the silicon region are maintained below atmospheric pressure by

drawing coolant through the detectors from an atmospheric pressure reservoir located slightly below the detector elevation.

# 4 Tracking resolution and B-physics capability

The resolution of the silicon tracker is determined largely by geometry, the pitch of the silicon detectors, and detector mass. While reconstruction techniques remain to be refined, we expect to make an initial reconstruction in the r-$\phi$ plane. All four silicon barrel axial layers have a trace pitch of 50 $\mu$m in this plane which leads to an expected $\sigma \approx 14$ $\mu$m for individual layers. The 2° stereo ladder surfaces in layers 2 and 4, while not used in initial track fits, should improve the trsnsverse resolutions of these layers by a factor of approximately $2^{-0.5}$ in final track fits. In a system where pulse height information is available, charge sharing between strips can be used to obtain further improvement.

The results of an early 2D impact parameter study, in which detector mass was approximated, are shown in Figure 6. The H-disks reduce the degradation in resolution which would otherwise occur above $\eta = 2.2$ as tracks begin to miss barrel layers.

A more recent, but still preliminary, GEANT study[6] has been made of ISAJET-generated events to better understand track residuals, impact parameter resolution, and triggering possibilities. Silicon strips were assumed to be 100% efficient and alignment was assumed to be perfect. In practice, detector alignment and our knowledge of detector positions may limit resolutions attainable. Using a track position based upon contiguous strips over threshold weighted by pulse height gave transverse resolutions of 6 $\mu$m to 8 $\mu$m in the barrel axial layers. Ignoring pulse height information and using just a strip average increased the resolution to about 12 $\mu$m. This more conservative resolution was used for the remainder of the study. Both the scintillating fiber tracker and the silicon tracker were included. At least one charged track or converted photon with $p_T$ above 1.5 GeV/c was required for an event to be retained. The impact parameter resolution obtained, 34 $\mu$m, compares acceptably with the expected transverse beam size of 40 $\mu$m and the average impact parameter for b-hadrons, about 140 $\mu$m. A test beam

program including a magnetic field is planned for the 1996 Fermilab fixed target run to verify silicon tracking resolutions.

In an independent study using MCFAST, R. Lipton and C.S. Mishra have examined the accuracy with which we can measure $\sin(2\beta)$ using the decay $B_d^\circ \rightarrow J/\psi\ K_S^\circ$. The results for three cases, $|\eta| < 1$, $|\eta_{trigger/reconstruction}| < 1$ with tagging to $|\eta| < 3$, and $|\eta| < 3$, are summarized in Table 4.

# 5 Conclusion

The design of the DØ silicon tracker is nearly complete. Silicon for the barrels has been ordered and prototype silicon has been received. The beryllium bulkhead designed has been completed and we are ready to purchase the bulkheads. We are prepared to embark on an aggressive fabrication schedule which will lead to completion, testing, and installation of the detector by mid-1999 for Run II of the Fermilab collider.

# 6 Acknowledgments

We thank the the U.S. Department of Energy, the U.S. National Science Foundation, and the Fermilab DØ Department, Research Division, and Accelerator Division for their support. All members of the DØ silicon tracking groups have contributed generously to the silicon tracker design. I particularly wish to thank Ron Lipton and John Ellison for work they have done on silicon design and B-physics, Shekhar Mishra for information he provided on expected accelerator operation and on B-physics, and Jadwiga Warchol, John Drinkard, Dave Stoker, and Greg Landsberg for work they have done on tracking resolutions and detector mass.

# References

[1] S. Abachi et al., Nucl. Inst. Meth. A338 (1994) 185.

[2] A.D. Bross, The DØ detector upgrade, 4th International Conference on Advanced Technology and Particle Physics, Como, Italy (1994).

[3] M.R. Wayne, The D0 tracker upgrade and projections for B physics, Nucl. Instr. Meth. A351 (1994) 77.

[4] The DØ Collaboration, The DØ upgrade, Fermilab (1995).

[5] DØ Upgrade Collaboration, DØ silicon tracker technical design report, Fermilab (1994).

[6] J. Drinkard and D. Stoker, An impact parameter trigger algorithm for the D0-$\beta$ detector, D0 note 2350, Fermilab (1994.)

| | |
|---|---|
| Start of physics run | Mid-1999 |
| Luminosity | $2 \times 10^{32}$ cm$^{-2}$sec$^{-1}$ |
| Luminosity lifetime | 4-6 hours |
| | (lifetime grows about 0.75 hours per hour) |
| Store duration | 6-10 hours |
| Integrated luminosity | 41 pb$^{-1}$/week |
| Interbunch spacing | 396 ns ($\geq$132 ns) |
| Length of interaction region | $\sigma \approx 10$ cm |
| | (growing to 20 cm during the first 4 hours) |
| Interactions per crossing | 5.3 |
| | (decreasing during store) |
| Transverse beam size | $\sigma \approx 40$ $\mu$m |

Table 1: Preliminary accelerator operating parameters for Run II

| Layer | Sublayer | Radius (mm) | Ladders | Active width (mm) | Single/double sided |
|---|---|---|---|---|---|
| 1 | Inner | 27.15 | 6 | 19.2 | Single |
| | Outer | 36.45 | 6 | 19.2 | Single |
| 2 | Inner | 45.50 | 6 | 32.0 | Double |
| | Outer | 55.54 | 6 | 32.0 | Double |
| 3 | Inner | 67.68 | 12 | 19.2 | Single |
| | Outer | 75.82 | 12 | 19.2 | Single |
| 4 | Inner | 91.01 | 12 | 32.0 | Double |
| | Outer | 100.51 | 12 | 32.0 | Double |

Table 2: Barrel ladders

| Element | Power dissipation | Number of elements | Total dissipation |
|---|---|---|---|
| Barrel | 276.5 | 7 | 1935.4 |
| F-disk | 122.9 | 12 | 1474.6 |
| H-disk | 184.3 | 4 | 737.3 |
| Total | | | 4147.2 |

Table 3: Design power dissipation (watts)

| | Central region | Central region plus full tag | Full detector |
|---|---|---|---|
| N produced in final state | 430,000 | 430,000 | 430,000 |
| $\varepsilon_{tag} \times \varepsilon_{accep} \times \varepsilon_{trig}$ | 0.0006 | 0.001 | 0.0034 |
| Number tagged | 236 | 492 | 1,443 |
| Dilution factor | 0.28 | 0.28 | 0.22 |
| Error in measurement | 0.24 | 0.16 | 0.12 |

Table 4: Determination of $\sin(2\beta)$ from $B \rightarrow J/\psi\ K_S$

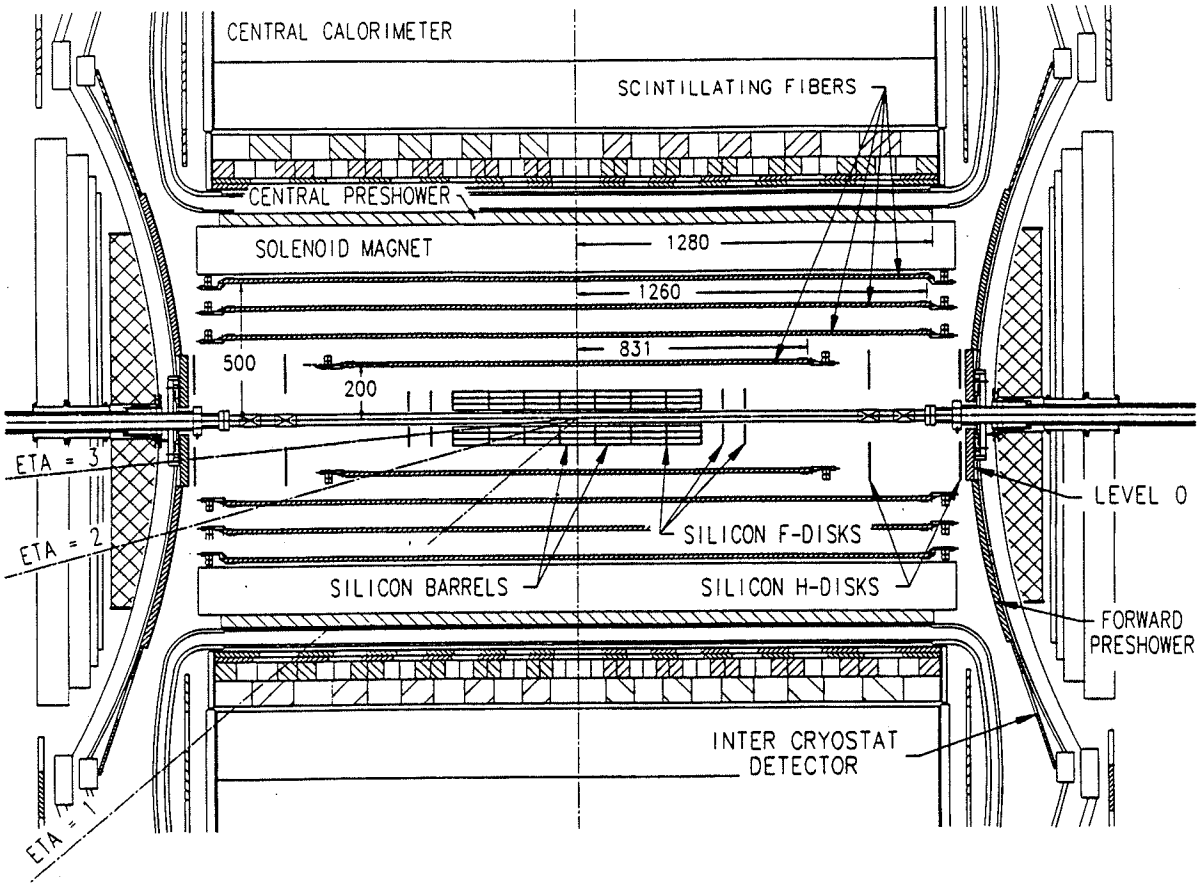


Fig. 1. $r$-$z$ view of the upgraded DØ detector central tracking region. The scintillating fiber barrels are supported from the ends of the solenoid cryostat. The silicon barrels and F-disks are supported from the innermost scintillating fiber barrel. Separate support is provided for the H-disks.

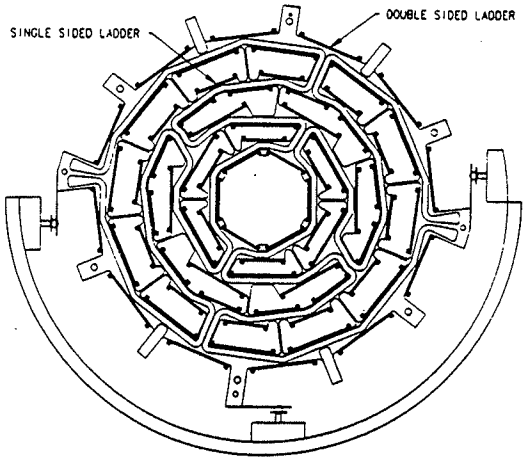


Fig. 2. $r$-$\phi$ view of a silicon barrel module. The 72 ladders are arranged in four layers, each with an inner and an outer sublayer. Coolant passages integral to the active beryllium bulkhead pass between inner and outer sublayers. Six mounting locations are provided for the associated F-disk. A carbon-fiber cable restraint ring is provided at the outer bulkhead radius, but has not been shown. The half-cylinder support structure is shown schematically. Its inner radius has been chosen to accommodate the physical radius of the F-disks.

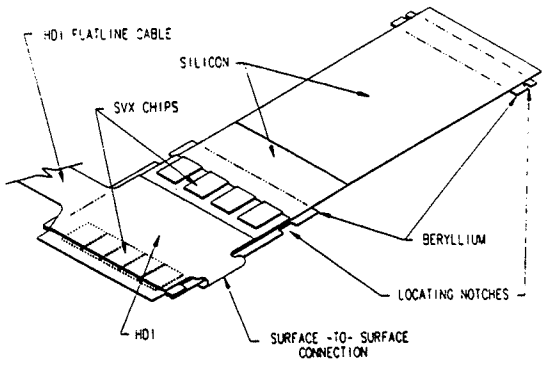


Fig. 3. The double-sided ladder design. 300 $\mu$m thick beryllium pieces provide positioning features at each bulkhead and act as substrates for the HDI at the active bulkhead. One row of SVX chips is mounted opposite the bulkhead mounting surface; a second set is near the end of the ladder. Two rails (not shown) are epoxied to the bottom surfaces of the two silicon detectors and to the two bottom beryllium pieces. Approximately 2600 wirebonds are required on each double-sided ladder.

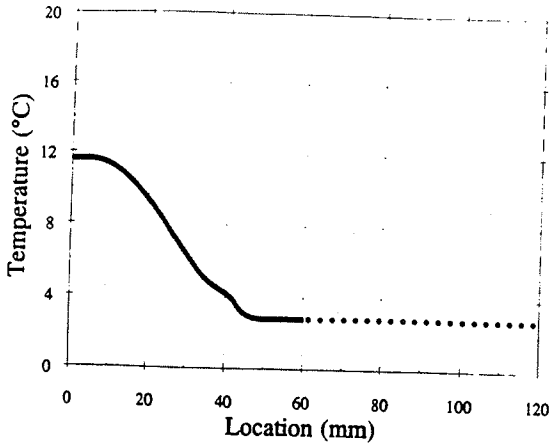


Fig. 4. The double-sided ladder silicon temperature. The bulkhead temperature has been taken to be 0°C in this calculation. Slightly less than 3°C temperature rise occurs in the epoxy joint between the bulkhead and the ladder. The silicon temperature rises about 9°C between the bulkhead location and the location of the SVX chips near the ladder end. Because our primary concern has been the silicon temperature at the readout end of the ladder, the temperature of the second (right) detector of the ladder has not been included in this calculation. Previous calculations have shown a rise of 1°C to 2°C between 60 mm and 120 mm as the result of detector leakage currents and convective heat transfer.

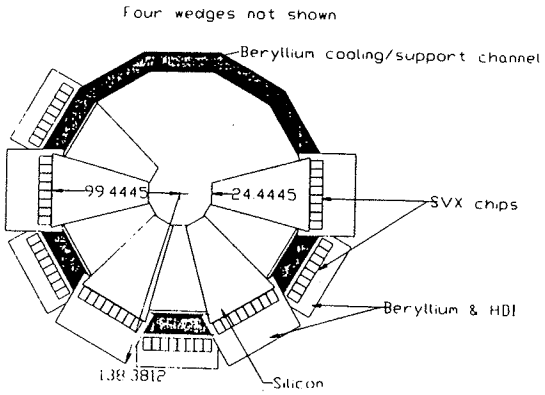


Fig. 5. F-disk geometry. A kapton flex-circuit jumper is used for connections between the silicon surface nearest the bulkhead and the readout HDI. Approximately 3600 wirebonds are required on each wedge.

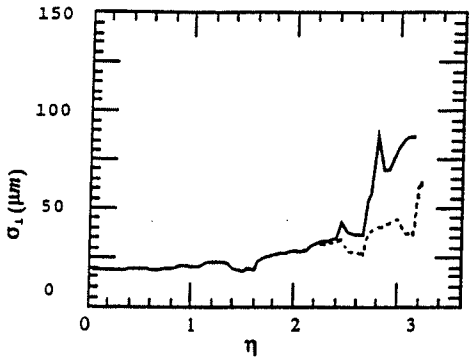


Fig. 6. Two-dimensional impact parameter resolution as a function of $\eta$ for 1 GeV/$c$ $p_T$ tracks. The resolution without H-disks is indicated by the solid curve. The dashed curve shows the resolution with H-disks.